Tzu Chi Medical Journal 2026; 38 (1): 11-20

Review Article

Development of an enhanced sensitivity method for lateral flow immunoassays: An overview of strategies

*Chung-An Chen[a,b], Chi-Hung Liu[a], Natalie Yi-Ju Ho[a], Sheng Liu[a], Tsung-Ting Tsai[a,b]**

[a]Department of Orthopaedic Surgery, Spine Section and Bone and Joint Research Center, Chang Gung Memorial Hospital, Taoyuan, Taiwan, [b]School of Medicine, Chang Gung University, Taoyuan, Taiwan

Submission : 23-Jul-2025
Revision : 03-Sep-2025
Acceptance : 07-Oct-2025
Web Publication : 13-Jan-2026

Abstract

Lateral flow immunoassay (LFIA) is a widely recognized point-of-care diagnostic platform for detecting various analytes. It must meet the criteria of REASSURED, but poor sensitivity and lack of precision in test results remain the main bottlenecks of LFIA. Therefore, signal enhancement methods, such as devices, nanoprobes, or detection modes, can improve this platform. In this paper, many representative studies from the past decade on LFIA sensing platforms will be discussed in detail.

Keywords: *Lateral flow immunoassay, Point-of-care, Sensing system*

Introduction

The gold standards of point-of-care test

The gold standards for diagnostic tools must encompass affordability, accessibility, and accuracy to ensure widespread application [1]. To address these requirements, the World Health Organization (WHO) has established criteria for diagnostic tools that are affordable, sensitive, specific, user-friendly, rapid and robust, equipment-free, and deliverable to end-users, collectively summarized by the acronym ASSURED [2,3]. Recent advancements in digital technology have expanded the ASSURED criteria into what is now known as REASSURED: Real-time connectivity, Ease of specimen collection, Affordable, Sensitive, Specific, User-friendly, Rapid and robust, Equipment-free, and Deliverable to end-users [4,5]. Among the technologies developed to meet REASSURED standards, lateral flow immunoassay (LFIA) stands out as one of the detection methods closest to achieving this goal [1,6].

The principle of lateral flow immunoassay

The configuration of the LFIA device consists of several components, including membranes such as the sample pad, conjugation pad, detection pad, and absorbance pad [Figure 1a]. The signal is generated through visible or fluorescent results from an immobilized captured reagent [7]. The sample pad controls the flow of the test solution, ensuring that the analyte in the sample binds with the capture reagents of the conjugates on the membrane [8]. If the target analyte is present, the labeled antibodies specific to it are conjugated with colored or fluorescent particles, most commonly gold nanoparticles (AuNPs) or latex microspheres. The concept is that the conjugated antibody binds with the target analyte. The test solution then migrates along the detection pad, which contains a porous membrane (typically nitrocellulose [NC]), where antibodies are immobilized on a test line (T-line) and a control line (C-line). The T-line indicates the recognition results, whereas the C-line confirms the proper liquid flow through the strip. Capillary action, supported by an absorbent pad, enables controlled fluid movement, wicking away excess reagents and preventing backflow. As a result, the varying intensities of the lines can be visually assessed with the naked eye or quantified using a dedicated reader [8,9].

Traditionally, LFIAs operate in two main formats: the sandwich format and the competitive format [2]. The sandwich format, which is more commonly used, is designed to detect target analytes using two antibodies that bind to different sites on the target molecule [6]. In contrast, the competitive format is often employed for detecting small analytes or single epitopes (such as chemicals or haptens) that lack suitable bioreceptor pairs [10]. Although competitive addresses some of these challenges, it typically generates a counterintuitive signal, where a weaker signal indicates a higher analyte concentration. This often results in ambiguous intermediate color intensities, which can be difficult for end users to interpret accurately with the naked eye, making semiquantitative analysis unreliable [10,11]. Therefore, this immunoassay platform benefits from flexible signal readout strategies that can enhance result

**Address for correspondence:* Dr. Tsung-Ting Tsai, Department of Orthopaedic Surgery, Spine Section, Chang Gung Memorial Hospital, 5, Fuxing Street, Guishan District, Taoyuan, Taiwan. E-mail: tsai1129@gap.cgu.edu.tw

This is an open access article distributed under the terms of the Creative Commons Attribution-NonCommercial-NoDerivatives 4.0 License (CC BY-NC-ND), where it is permissible to download and share the work provided it is properly cited. The work cannot be changed in any way or used commercially without permission from the journal.

For reprints contact: WKHLRPMedknow_reprints@wolterskluwer.com

How to cite this article: Chen CA, Liu CH, Ho NY, Liu S, Tsai TT. Development of an enhanced sensitivity method for lateral flow immunoassays: An overview of strategies. Tzu Chi Med J 2026;38(1):11-20.

Access this article online
Quick Response Code:
Website: www.tcmjmed.com
DOI: 10.4103/tcmj.TCMJ-D-25-00061

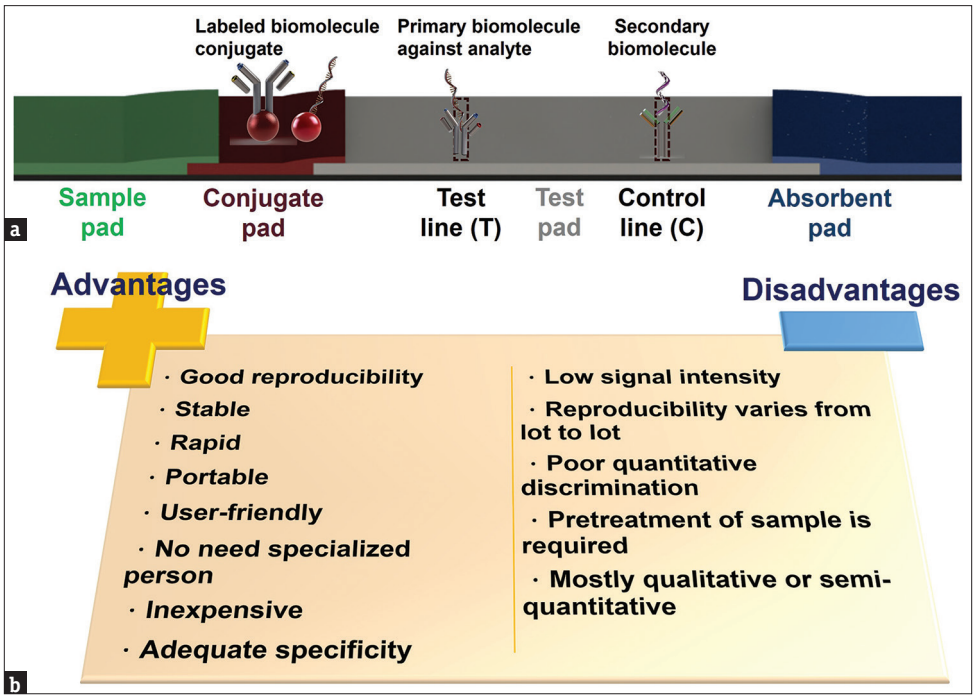

Figure 1: The basic structure (a), the advantages and disadvantages (b) of lateral flow immunoassay

interpretation and support more user-friendly designs [11]. When comparing the two formats, the sandwich format generally offers higher analytical sensitivity. It is often capable of detecting analyte concentrations in the picogram per milliliter range, compared to the nanogram per milliliter range typically observed in competitive assays [12]. However, the sandwich format can be susceptible to false-negative results due to the "high-dose effect" (Hook effect) at elevated analyte concentrations, a limitation generally avoided in competitive assay designs [13,14]. Each format presents distinct advantages and limitations depending on the nature of the target analyte, its relevant concentration range, and the intended purpose of the test system [12].

In addition, LFIAs have widespread applications across various settings and have been successfully employed to detect a broad range of target antigens, from atoms to whole cells, in diverse sample types [7]. These applications include the detection of hormones [15], infectious pathogens [3,16-19], diseases or cancer biomarkers [2,20-23], chemical compounds, and poison or pesticide residues [24-28], among others. Compared to standard laboratory technologies, LFIA offers several advantages, such as ease of use, speed, low cost, and portability, making it particularly suitable for health care in resource-limited settings. It is also applicable in a variety of fields, including clinical biomedicine [29,30], environmental pollutant analysis [31,32], food [33,34], and drug safety [35,36]. However, one limitation of LFIA is its relatively low sensitivity for detection [37,38]. To address this, numerous studies have proposed various designs aimed at enhancing the signal to improve detection sensitivity [39]. The basic structure, advantages, and disadvantages of lateral flow assays are summarized in Figure 1. This review examines and compares different methods developed to enhance sensitivity within the LFIA platform.

The structures with sensitivity enhancement components for the design of lateral flow immunoassay devices

To enhance sensitivity, modifying the architecture of the LFIA platform can be an effective research strategy for improving detection performance. One approach to increasing sensitivity involves the design and integration of components [Table 1]. For example, Fu *et al*. developed a simple three-inlet two-dimensional paper network (2DPN) that utilizes AuNP labeling and a gold enhancement solution to achieve signal amplification and improve the limit of detection (LoD). This design produced an initial signal of approximately 6.4 counts above background, due to the capture of streptavidin–gold conjugates on the surface. The addition of the gold enhancement solution amplified the signal to around 46 counts above background, resulting in a signal amplification ratio of approximately 7.3 [40]. One year later, Fu *et al.* developed a paper network platform that extends the conventional lateral flow assay into two dimensions, allowing the integration of multistep processes to enhance sensitivity while preserving the advantages of traditional lateral flow tests. They modified a commercial strip test for detecting human chorionic gonadotropin (hCG) in pregnancy tests, demonstrating an almost four-fold improvement in the LoD compared to conventional lateral flow assays. The 2DPNs showed significant potential, offering a cost-effective, user-friendly alternative to conventional lateral flow strips. This platform enables the automated, sequential delivery of multiple reagents to the detection region with a single user activation step [41].

Table 1: Comparison of different components for the sensitivity enhancement of the lateral flow immunoassay

The modification part	Target analyte	Sample matrix	Sensing mode	LoD	Assay time (min)	Reference
2DPN	BSA	Water	Colorimetric	Average signal amplification ratio of~5.9±1.8	20	[40]
2DPN	hCG	Spiked into FBS	Colorimetric	0.3±0.2 mIU/mL	35	[41]
Dialysis-based concentration method	Nucleic acid (HIV) Protein (myoglobin)	Spiked into the PEG solution	Colorimetric	0.1 nM 1.56 ng/mL	25	[42]
Stacking pad	Protein A CRP	Serum or synovial fluid samples into PBS buffer	Colorimetric	1 ng/mL 15.5 ng/mL	20	[43]
Stacking pad with mLFIA	CRP Alpha-defensin	Synovial fluid sample mixed with AuNPs conjugated solution	Colorimetric	5 µg/mL 10 µg/mL	20	[44]
SSM	SARS CoV-2 N protein	2%–5% (w/w) bovine serum albumin solution	Colorimetric Fluorometric	3.98 pg/mL 53.3 fg/mL	3.5	[45]
Core–shell hybrid nanofibers and silver-reducing reagents in the core	cTnI	Spiked into human serum	Colorimetric	0.24 ng/mL	20	[46]
Two independent sample inlets	Ferritin	Human serum sample	Colorimetric	0.03 and 0.05 ng/mL	10	[47]
Copper depositing on AuNPs at the test line	Protein A Exotoxin A	Synovial fluid into PBS buffer	Colorimetric	3 ng/mL 10 ng/mL	20	[48]

2DPN: Two-dimensional paper network, SARS CoV-2: Severe acute respiratory syndrome coronavirus 2, BSA: Bovine serum albumin, hCG: Human chorionic gonadotropin, CRP: C-reactive protein, LoD: Limit of detection, AuNPs: Gold nanoparticles, mLFIA: Multimodal lateral flow assay, HIV: Human immunodeficiency virus, cTnI: Cardiac troponin I, SSM: Spike, membrane nucleocapsid, PEG: Polyethylene glycol, PBS: Phosphate-buffered saline, FBS: Fetal bovine serum

With a novel pad design, Tang *et al*. developed a dialysis-based concentration method integrated into the sample pad of an LFIA device. This system successfully achieved a 10-fold increase in sensitivity for nucleic acid detection (human immunodeficiency virus [HIV]) and a 4-fold enhancement in protein detection (myoglobin) [42]. Tsai *et al*. introduced an additional stacking pad component in their stacking LFIA (sLFIA) design to concentrate antibodies and antigens [43], inspired by the stacking gel used in polyacrylamide gel electrophoresis. This design enhances protein concentration, increasing antibody–antigen interaction time and improving assay performance. Clinical testing with human serum and synovial fluid samples demonstrated that the sLFIA platform achieved a 1.2- to 1.7-fold increase in sensitivity compared to traditional LFIA. Furthermore, this simple design was extended to a multitarget LFIA strip for diagnosing periprosthetic joint infections [44]. Liu *et al.* proposed a surface structure membrane (SS Mem), which facilitates rapid water transport through convection and minimizes sample residue on the membrane after flow. This innovation addresses several limitations of conventional LFIA, such as low sample flow velocity and higher sample residuals. The SS Mem achieved a 7.1-fold increase in flow velocity and reduced sample residuals by 60%–67%, compared to the NC Mem. When used in a nanogold LFIA for detecting the severe acute respiratory syndrome coronavirus 2 (SARS-CoV-2) nucleocapsid protein, the SS Mem required only 210 seconds of waiting time, with a LoD of 3.98 pg/mL and 53.3 fg/mL, 96.5% sensitivity, and 90% specificity. These results suggest that LFIA platforms utilizing the SS Mem hold significant potential for broadening applications in biosensing [45].

To integrate enhancement methods with membranes or films, Kim *et al*. developed a straightforward approach to improve the sensitivity of LFIA using core–shell hybrid nanofibers. These nanofibers consisted of a water-soluble polymer shell and silver-reducing reagents in the core. The nanofibers were fabricated using a coaxial electrospinning technique and directly deposited onto the NC membrane in front of the test line (T-line). The platform was designed such that the AuNPs at the test line could interact with silver enhancement reagents released from the nanofibers. This process reduced silver ions to metallic silver around the AuNPs, darkening the color of the test line. To validate this design, various concentrations of troponin I (TnI) were spiked into human serum, resulting in the reduction of silver ions to metallic silver, which further darkened the test line. The hybrid nanofiber concept significantly enhanced the detection limit of a commercial LFIA, improving sensitivity by up to 10 times, while maintaining the convenience of the analysis [46]. Preechakasedkit *et al.* introduced a novel device to enhance the sensitivity of AuNPs-based LFIA by incorporating two independent sample inlets. The platform combined a low-cost adhesive tape with a hydroxylamine/polyvinyl alcohol/polyethylene oxide blend film. After optimizing the conditions, the ferritin detection using the AuNPs' enhancement (LOD = 0.5 ng/mL) and the double-sample inlet device (LOD = 2 ng/mL) demonstrated 20-fold and five-fold increases in sensitivity, respectively, compared to conventional devices, confirming the improvement in sensitivity [47]. Chien *et al.* introduced a novel one-step copper deposition-induced signal amplification LFIA (osa-LFIA), which significantly enhances detection sensitivity for protein A and exotoxin A in bacterial analysis. The osa-LFIA provided a 10-fold improvement over conventional LFIA, lowering the LoD to 3 ng/mL for protein A and 10 ng/mL for exotoxin A, respectively [48].

Nanotechnology enhancement methods by nongold nanoparticle system

Recently, a variety of novel nanomaterials have been used as signal transducers or receptors in LFIA platforms, successfully enhancing their analytical capabilities for diagnostic applications [49]. This paper introduces and focuses on various nongold nanoprobe reporters to enhance LFIA platforms, including colorimetric, fluorometric, and chemiluminescent (CL) methods [Table 2]. For the colorimetric approach, Loynachan *et al*. reported the use of porous platinum core–shell nanocatalysts (PtNCs), which demonstrated high catalytic activity when exposed to complex human blood serum samples. By pairing porous catalytic inorganic nanoparticles (NPs) with thermally stable antibody fragments containing easily modifiable functional groups, they successfully enhanced sensitivity in the LFIA platform. This approach enabled catalytic amplification using PtNCs to detect p24 spiked into serum at femtomolar concentrations (approximately 0.8 pg/mL) and acute-phase HIV in clinical human plasma samples in under 20 min [50]. Su *et al*. developed a novel LFIA biosensor by incorporating CO_3O_4 NPs as signal labels for the detection of 3-amino-2-oxazolidinone (AOZ), a metabolite of furazolidone. This approach achieved a detection limit of 0.4 ng/mL for AOZ, demonstrating at least three times greater sensitivity compared to conventional AuNP-based LFIA [51]. Kim *et al*. developed silica-coated silver-assembled silica NPs (SiO_2@Ag@SiO_2 NPs) for use in a visual LFIA platform to detect prostate-specific antigen (PSA). The LoD of the test strip using SiO_2@Ag@SiO_2 NPs was 1.1 ng/mL, approximately two and a half times more sensitive than the conventional colloidal AuNPs-based LFIA [52]. Liang *et al*. developed a multimodal lateral flow assay (mLFIA) by combining the catalytic sites of copper (Cu) NPs with an inherent photothermal polydopamine (PDA) scaffold in a one-step process, creating an efficient signal element. The resulting compact and robust Cu-anchored PDA (PCu) exhibited peroxidase-mimicking and photothermal properties, enabling simultaneous triple signal readouts for colorimetric, amplified colorimetric, and photothermal detection of target analytes. This study demonstrated the detection of Aspergillus flavus, achieving accurate and sensitive detection with concentrations as low as 0.45 and 0.22 ng/mL, representing 19- and 40-fold improvements over traditional colorimetric methods. This

Table 2: Comparison of different sensing modes and nanomaterials for the sensitivity enhancement of lateral flow immunoassay

Sensing modes	Nanoreporters	Targets	Sample matrix	LoD	Assay time (min)	Reference
Colorimetric	PtNCs	p24	Human plasma sample	0.8 pg/mL	20	[50]
	Co_3O_4 NPs	Furazolidone	Water	0.4 ng/mL	6	[51]
	SiO_2@Ag@SiO_2 NPs	PSA	Human serum sample	1.1 ng/mL	10	[52]
	CuNPs	*Aspergillus flavus*	Powder dissolved into PBS	0.45 ng/mL	~13	[53]
	LiAGNPs	IgG/IgM	Spiked into FBS sample	31.3/7.8 ng/mL	15	[54]
	MPBN	RAC/CLE	Spiked into water	0.12/0.2 ng/mL	10	[55]
	DMSN	DMSN	Spiked into PBS with BSA	0.52 ng/mL	7	[56]
Fluorometric	FNDs	HIV-1 RNA	Seroconversion panel	120 fM	~30	[57]
	MQBs	Influenza A virus	Spiked into IAV virions	22 pfu/mL	10	[58]
	ACNPs	β-lactam	Real milk sample	1–100 ng/mL[a]	5n	[59]
	LiAGNPs	p24	Spiked into serum sample	0.006 ng/mL	15	[54]
		IgG/IgM (SARS-CoV-2)	Spiked into the FBS sample	15.6/3.9 ng/mL (FL) 0.98/0.24 ng/mL (afterglow signal)		
	Peroxyoxalate-based fluorescent particle	hCG	Serum from healthy donors	39 pg/mL	15	[60]
		N protein (SARS-CoV-2)	Self-collected nasal swab specimen and saliva	100 pg/mL		
	ACNPs	SA	Sample from the local market	2 ng/mL	~10	[61]
	UCNPs	CRP	Serum sample	0.046 ng/mL	15	[62]
Chemiluminescence	PSNPs	H9N2	Cloacal swab sample	$10^{3.5}$ EID_{50}/mL	20	[63]
		H1N1		$10^{2.5}$ EID_{50}/mL		
		H5N9		10^{4} EID_{50}/mL		
	CoFe PBAs/WS2	GM	Spiked into milk, urine, and serum	0.33 pg/mL	15	[64]
Photothermal	DMSN	PSA	Working buffer (PBS within BSA)	0.202 ng/mL	<10	[56]

[a]The cutoff values against ampicillin, amoxicillin, benzylpenicillin, dicloxacillin, cloxacillin, oxacillin, nafcillin, cefquinome, cefoperazone, cefapirin, ceftazidime, cephalothin, cefepime, cefoxitin, cefazolin, ceftriaxone, ceftiofur, cefotaxime, cefalexin, imipenem, meropenem, and ertapenem were 1, 2, 2, 10, 10, 10, 10, 3, 3, 3, 5, 10, 10, 20, 20, 20, 30, 30, 100, 10, 15, and 15 ng/mL, respectively. LoD: Limit of detection, IAV: Influenza A virus, ACNPs: Amorphous carbon nanoparticles, hCG: Human chorionic gonadotropin, DMSN: Dendritic mesoporous sili, CRP: C-reactive protein, BSA: Bovine serum albumin, CLE: Clenbuterol, RAC: Ractopamine, LiAGNPs: Dye-energized light-initiated afterglow nanoprobes, MQNs: Magnetic quantum dot nanobeads, MPBN: Magnetic Prussian blue nanozyme, NPs: Nanoparticles, HIV: Human Immunodeficiency Virus, EID_{50}: 50% egg infective dose, FNDs: Fluorescent nanodiamonds, SARS CoV-2: Severe acute respiratory syndrome coronavirus 2, PtNCs: Platinum core–shell nanocatalysts, PBS: Phosphate-buffered saline, PSA: Prostate-specific antigen, PSNPs: Porous silica nanoparticles, UCNPs: Upconversion nanoparticles, IgG: Immunoglobulin G, IgM: Immunoglobulin M, MQBs: Magnetic quantum dot nanobeads, FBS: Fetal bovine serum, SA: Sulfonamide, GM: Gentamicin

research presents an efficient peroxidase-mimicking and photothermal multifunctional nanomaterial for use in a visual mLFIA platform, enhancing analytical capabilities [53].

Fluorescent detection is a popular method in platform design, a phenomenon first observed by Herschel in 1845 when he discovered fluorescence in quinine water [65]. The fluorescence mechanism involves a molecule absorbing light at a specific frequency, followed by relaxation to a lower energy state (typically the ground state) through the emission of a photon, without any change in electron spin [66]. Due to its high sensitivity and specificity to the microenvironment, fluorescence emission holds great potential for the development of biosensing applications [67]. Among these substances, NP-based fluorescent materials have exhibited numerous interesting properties, making them the focus of intense research [68]. Therefore, NP-based fluorescent systems offer improved sensing and molecular diagnostic designs, expanding their functionality and positioning them as promising alternatives to organic fluorophores. To date, NP-based fluorescent sensing platforms have proven to be valuable tools for detecting sensitive biological reactions and sensing biomolecules at ultralow concentrations, which is difficult to achieve with traditional organic fluorophores. Miller *et al*. demonstrated the use of fluorescent nanodiamonds (FNDs) as a fluorescent label for an LFIA platform, enabling efficient signal separation from background noise in the frequency domain through lock-in detection. This platform introduced the first FND-based LFIA system for molecular HIV-1 RNA assays, achieving a detection limit of 8.2×10^{-19} molar for a biotin–avidin model, which was 10^5 times more sensitive than gold NP-based detection, highlighting its potential for clinical applications [57]. Bai *et al*. developed a magnetic quantum dot nanobeads (MQBs)-based lateral flow assay (LFA) for detecting influenza A virus (IAV) virions in clinical specimens, utilizing magnetic enrichment and fluorescent detection. The IAV-specific antibody was conjugated with MQBs to capture IAV virions and serve as highly bright fluorescent probes on lateral flow strips. This platform achieved a low LoD of 22 pfu/mL within 35 min and demonstrated good specificity in distinguishing between influenza B virus and two adenovirus strains [58]. Zhang *et al.* developed a highly sensitive LFIA to detect 22 β-lactams using a high-sensitivity label and an indirect labeling format. In this novel approach, β-lactam receptors were used without labeling, whereas antireceptor monoclonal antibodies (mAbs) were labeled with amorphous carbon NPs. The results demonstrated significantly higher sensitivity, with cutoff values 2-fold lower than those using colloidal gold labels, and 10-fold lower than the conventional receptor-CG-LFIA format [59]. Hao *et al*. reported a novel aggregation-induced emission (AIE) dye-energized light-initiated afterglow nanoprobes (LiAGNPs) with remarkable time-resolved luminescence properties, demonstrating their potential for the sensitive detection of infectious diseases on test strips. They selected HIV and SARS-CoV-2 as models for LFIA validation. The LiAGNPs-based LFIA platform showed 2-fold and 32-fold greater sensitivity than the currently used Eu (III)-based time-resolved fluorescent NPs and AuNPs, respectively, while maintaining sensitivity and offering greater application flexibility [54]. Brosamer *et al*. demonstrated a chemical excitation system that replaces the optical excitation of standard fluorescent NPs by utilizing peroxyoxalate-based chemistry from inexpensive, shelf-stable glowsticks. This LFIA sensing system successfully detected hCG with a LoD of 39 pg/mL and was also applied to detect the SARS-CoV-2 nucleoprotein at 100 pg/mL in nasal swab extracts [60]. Dang *et al*. developed an LFIA utilizing amorphous carbon nanoparticles (ACNPs) conjugated with mAbs to screen for sulfonamide (SA) residues, with high sensitivity toward sulfamethazine (SM2) in milk samples. This LFIA was able to detect SA with a cutoff value of 2 ng/mL for SM2, meeting the required sensitivity for sulfonamide detection [61]. Jin *et al*. developed a simple and versatile method to optimize upconversion nanoparticle (UCNP)-based LFIA by integrating it with a homemade benchtop fluorescence analyzer. For C-reactive protein (CRP) detection, the system achieved nearly a 20-fold increase in sensitivity, with a LoD of 0.046 ng/mL and a broad detection range of 0.2–300 ng/mL. This concept holds promise for optimizing other nanoparticle-based bioprobes and integrating them with homemade benchtop fluorescence analyzers for widespread point-of-care testing (POCT) applications [62].

CL assays do not require an external excitation light source, which helps eliminate interference or background signals from the sample matrix, resulting in a high signal-to-noise ratio. This allows for a wide linear range with over five decades of concentration sensitivity [69]. Jung *et al*. developed a signal-amplifiable nanoprobe-based CL-LFIA using size-selective immobilization of antibodies (binding receptors) and enzymes (signal transducers) on signal-amplifiable nanoprobes. The LoD of the CL-LFIA using porous silica NPs for detecting the nucleoprotein of the H3N2 virus was 5 pM. Sensitivity tests for H9N2, H1N1, and H5N9 showed values of 103.5, 102.5, and 104.5 50% egg infective dose (EID50)/mL, respectively, which were 20 to 100 times lower than those achieved by a commercial AIV rapid test kit. This CL-LFIA platform demonstrated high sensitivity and specificity in detecting 37 clinical samples, highlighting its potential as an ultrahigh-sensitivity diagnostic tool for clinical applications [63]. Wu *et al*. developed a novel, highly sensitive, and portable LFIA based on CoFe PBAs/WS2 nanozyme-mediated chemiluminescence (CL) for POCT biosensing of gentamicin (GM). The dynamic detection range of the CL-LFIA system extended from 1 pg/mL to 100 ng/mL, with a LoD of 0.33 pg/mL. The assay could be completed in just 15 min. Recovery rates for GM spiked into complex matrices, including milk, urine, and serum, ranged from 90.94% to 109.74%, demonstrating the reliability and applicability of the CL-LFIA for real sample analysis [64].

Nanozymes are a new generation of artificial enzymes that offer advantages such as high catalytic activity, good stability, low cost, and the unique properties of nanomaterials [70]. Recently, a surge of nanozymes has been demonstrated to catalyze typical enzymatic reactions, mimicking radicals such as O_2^-, O_2^{2-}, OH, OOH, as well as enzymes such as catalase and hydrogen peroxide (H_2O_2) catalysis [70,71]. It not only

offers opportunities for environmental protection and healthcare treatment but also enables multipurpose sensing and imaging platforms for LFIA design and detection [72]. Liu *et al*. developed a magnetic Prussian blue (PB) nanozyme-mediated dual-readout on-demand multiplex LFIA (mLFIA) for the analysis of ractopamine (RAC) and clenbuterol (CLE). The recoveries ranged from 84.01% to 119.94%, demonstrating repeatability and reliability. The calculated LoD for the dual-readout mLFIA was 0.12 ng/mL for RAC and 0.20 ng/mL for CLE. This method utilized nanozymes as ideal signal donors, showing significant potential for monitoring other targets [55]. Gong *et al.* developed a nanozyme by *in situ* growing PB within the pores of dendritic mesoporous silica nanoparticle (DMSN), which increased the exposure of active sites and enhanced the peroxidase (POD)-like activity of the LFIA sensing system. The antibody-modified DMSN@PB nanozymes provided enzymatic-enhanced colorimetric and photothermal dual-signal functions for detection. After systematic optimization, the DMSN@PB-LFIA demonstrated a 4-fold amplification of the colorimetric signal within 7 min, exhibiting a wide linear range (1–40 ng/mL) and a low LoD of 0.202 ng/mL for PSA analysis. This research offers a more accurate and reliable visual analysis methodology for the early diagnosis of prostate cancer, a key biomarker [56].

From the optical or thermal enhancement mode for the detection

Overall, the performance of LFIA sensing methods can be improved through the construction of devices, integration of nanotechnology, and selection of appropriate detection modes [Table 3]. Surface-enhanced Raman spectroscopy (SERS) offers a promising approach for enhancing the accuracy and sensitivity of LFIA [82,83]. In addition, the phenomenon of fluorescence resonance energy transfer (FRET) is highly effective in reducing background noise and enhancing signal detection [84]. On the other hand, the thermal contrast amplification (TCA) method, which combines nanomaterials, has been developed as a novel analytical approach in LFIA [85].

SERS provides rich chemical fingerprint information through Raman spectroscopy and enhances sensitivity through plasmon-enhanced excitation and scattering [86]. It can be conveniently used for detection under ambient and aqueous conditions, making it ideal for studying complex biological systems and attracting increasing interest in bio-related analysis [86,87]. Zhang *et al*. developed a lateral flow assay using core–shell SERS nanotags for the multiplex and quantitative detection of cardiac biomarkers, aiming at the early diagnosis of acute myocardial infarction. Specifically, Raman dyes were embedded within the gap between a silver core and gold shell, creating SERS nanotags to serve as labels instead of traditional gold colloids. As a result, the LoDs for cardiac enzymes, including Myo, cardiac troponin I (cTnI), and CK-MB, were below their clinical cutoff values, at 3.2, 0.44, and 0.55 pg/mL, respectively. The linear dynamic ranges for Myo, cTnI, and CK-MB were 0.01–500 ng/mL, 0.01–50 ng/mL, and 0.02–90 ng/mL, respectively, covering the clinical concentration ranges of these biomarkers in the human body [73]. Jia *et al*. designed SERS-LFIA biosensor strips using SiO2@Au NPs to enable highly sensitive and specific detection of ricin, staphylococcal enterotoxin B, and botulinum neurotoxin type A. These new strips exhibited sensitivity 100 times higher than that of colloidal gold-based LFIA strips [74]. González-Cabaleiro *et al*. integrated a digital SERS-based LFIA for the detection of SARS-CoV-2 nucleocapsid (N) protein, implementing an accurate and ultrasensitive quantitative sensing approach. This study demonstrated a quantification range for the viral protein in nasal swabs from 0.001 to 10 pg/mL, with a LoD as low as 1.9 aM (0.9 fg/mL), significantly enhancing the performance of

Table 3: Comparison of surface-enhanced Raman spectroscopy, fluorescence resonance energy transfer, and thermal contrast amplification detection mode for sensitivity enhancement of lateral flow immunoassay

Detection mode	Target analytes	Signal reporter	Sample matrix	LoD	Assay time (min)	Reference
SERS	Myo, cTnI, and CK-MB	Silver core and gold shell NPs	Spiked into serum	3.2, 0.44, and 0.55 pg/mL	7	[73]
	Ricin, SEB, and BoNT/A	SiO_2@Au NPs	Spiked into orange juice, apple juice, and milk	0.1, 0.05, and 0.1 ng/mL	15	[74]
	SARS-CoV-2 N protein	Au@Ag NPs	Spiked into nasal swab	1.9 aM (0.9 fg/mL)	30	[75]
FRET	cTnI	Absorbers: GNR Fluorescers: Europium chelate-contained silica NPs	Spiked into serum	97 pg/mL	>20	[76]
	T-2 toxin	Absorbers: AuNPs and ACNPs Fluorescers: QDs	Spiked into the cereal sample	1 and 0.22 ng/mL	<15	[77]
TCA	Influenza, malaria, and *Clostridium difficile*	AuNPs	Blood diluted by buffer or saline	~4–8-fold sensitivity enhancement	~10	[78]
	p24 protein	AuNPs	Spiked into human serum	8 pg/mL	~10	[79]
	Escherichia coli O157:H7	rGO	Spiked into milk	5×10^5 CFU/mL	20	[80]
	-	Silica-core GNSs	-	~57-fold sensitivity enhancement	-	[81]

GNSs: Gold nanoshells, GNR: Gold nanorod, rGO: Reduced graphene oxide, SERS: Surface-enhanced Raman spectroscopy, FRET: Fluorescence resonance energy transfer, TCA: Thermal contrast amplification, NPs: Nanoparticles, SARS-CoV-2: Severe acute respiratory syndrome coronavirus 2, SEB: Staphylococcal enterotoxin B, QDs: Quantum dot nanospheres, ACNPs: Amorphous carbon nanoparticles, LoD: Limit of detection, BoNT/A: Botulinum neurotoxin type A, AuNPs: Gold nanoparticles, cTnI: Cardiac troponin I, CK-MB: Creatine Kinase-Myocardial Band

traditional LFIAs and conventional SERS-based LFIAs. The integration of LFIA and digital SERS enables ultrasensitive detection of microbes and disease biomarkers [75].

The FRET phenomenon typically involves two fluorescent chromophores: a donor and an acceptor, a concept first proposed by Theodor Förster in 1948 [88]. In this process, the donor and acceptor must be positioned within an optimal distance (approximately 2–10 nm). When this condition is met, nonradiative energy transfer occurs between the donor and acceptor, resulting in a decrease in the donor's fluorescence intensity and an enhancement in the fluorescence of the acceptor [89]. FRET is a highly valuable technique with broad applications in biomedicine, pharmacology, toxicology, and food sciences [90]. Lee *et al*. developed a time-resolved-FRET technique integrated with a Fusion 5 membrane in an LFIA system for detecting cTnI in serum. This platform was designed without the need for additional sample or conjugation pads, simplifying the process and making it cost-effective. The system achieved a LoD of 97 pg/mL in human serum, using a single matrix (the Fusion 5 membrane) for cTnI diagnosis, thus streamlining the manufacturing process [76]. Zhang *et al*. enhanced the sensitivity of LFIA by adopting a conventional competitive format combined with a "turn-on/off" mode. They used AuNPs and amorphous carbon nanoparticles (ACNPs) as absorbers, whereas quantum dot nanospheres and time-resolved fluorescent microspheres (TRFMs) were selected as fluorophores for the "turn-on" mode LFIA. After optimization and comparison, the ACNPs-mAb-TRFMs-BSA system showed the highest sensitivity, offering a promising approach to improve LFIA performance for on-site screening of trace substances [77].

The principle of TCA leverages the localized surface plasmon resonance of AuNPs, which are tuned to match the wavelength of the laser. This allows AuNPs to efficiently convert light energy (photons) into heat. By utilizing this heat generation from AuNPs, TCA integrates thermography techniques, offering potential diagnostic applications [91]. Wang *et al*. developed a TCA reader to address the challenges of low sensitivity and lack of quantification in LFIAs. This TCA reader enhanced the analytical sensitivity by approximately eightfold and enabled quantification across LFIA tests for influenza, malaria, and *Clostridium difficile*. The reader integrated a laser, infrared camera, and other components, demonstrating high potential for POCT applications [78]. Zhan *et al*. developed and optimized a TCA-LFIA for the detection of HIV p24 protein, enabling ultrasensitive detection at 8 pg/mL in human serum. This study introduced several innovations, including: (a) defining a new quantitative figure of merit for LFIA design based on the specific-to-nonspecific binding ratio (BR); (b) applying different sizes and shapes of AuNPs to optimize the TCA-LFIA system; and (c) testing new laser wavelengths and power regimes for improved TCA-LFIA performance [79]. Vahid Shirshahi *et al*. reported on the photothermal properties of reduced graphene oxide (rGO) to enhance the signal in LFIAs for the detection of *E. coli* O157:H7 as a model pathogen. This sensing platform established a calibration curve for the photothermal method, which exhibited a linear range from 5×10^5 to 5×10^7 CFU/mL, with a correlation coefficient (R^2) of 0.96 for standard bacterial solutions in phosphate buffer. The LoD was approximately 5×10^5 CFU/mL for standard bacterial solutions, representing a 10-fold improvement in sensitivity compared to qualitative results. Therefore, this approach demonstrated strong potential for rapid detection and fast quantitative results with improved sensitivity [80]. Liu *et al.* explored the limits of TCA reading for AuNPs (AuNPs/mm^2) in the test regions of LFIA. They employed continuous-wave (CW) and millisecond pulsed lasers to establish a rapid TCA sensing system. This system achieved a 10- to 20-fold improvement in sensitivity over visual reading by using silica-core gold nanoshells preloaded in NC membranes to enhance the LoD for LFIA [81].

Comparison with clinical gold standards

While LFIAs have made significant technological advancements in recent years, several challenges remain to be addressed before they can be considered a gold standard in clinical diagnostics. Key limitations include relatively low sensitivity, limited measurement accuracy, and the absence of uniform industry standards [92]. Despite notable progress, LFIA performance can still be affected by various factors such as sample type and condition, preparation methods, sample volume, pH, analyte concentration, and weak interactions between the analyte and recognition elements [93,94]. Although LFIAs are increasingly being adopted in point-of-care and daily diagnostic applications, a number of issues must be resolved to ensure their broader clinical reliability and acceptance [92], including the following: (1) breakthroughs in sensitivity and multiplex detection; (2) innovation in capture elements; (3) portable and intelligent upgrades; (4) integration with multitechnology platforms; and (5) development of green and cost-effective solutions. Currently, LFIA platforms and electrochemical sensors are best suited for rapid, on-site screening. Their most rational application lies in mass screening of at-risk populations or asymptomatic individuals [12,92]. For situations requiring high sensitivity and precision, established gold-standard techniques such as PCR, ELISA, or SERS remain the preferred methods. These conventional assays also serve as reference standards for validating the performance of newer sensor technologies [92].

Conclusions

LFIA is a rapid, easy-to-use, and cost-effective sensing method for in-field diagnostics, particularly in resource-limited areas. However, it has long-standing criticisms, including low sensitivity, low specificity, and a lack of quantification capabilities [95,96]. To address these limitations, numerous studies have proposed various designs, incorporating changes in structure, materials, and labels, which are critically evaluated in this review. The specificity of LFIA is crucial for achieving ultrasensitive (aM) detection in POCT diagnostics. As these challenges and limitations are overcome in the future, the potential of LFIA is expected to grow, with improvements such as smaller sample volumes, shorter analysis times, elimination of the hook effect, and enhanced accuracy and sensitivity, ultimately supporting large-scale POCT applications.

Data availability statement

Data sharing is not applicable to this article as no datasets were generated or analyzed during the current study.

Financial support and sponsorship

Nil.

Conflicts of interest

There are no conflicts of interest.

References

1. Klebes A, Kittel AS, Verboket RD, von Stetten F, Früh SM. Multianalyte lateral flow immunoassay for simultaneous detection of protein-based inflammation biomarkers and pathogen DNA. Sens Actuators B Chem 2022;355:131283.
2. Mahmoudi T, de la Guardia M, Baradaran B. Lateral flow assays towards point-of-care cancer detection: A review of current progress and future trends. TrAC Trends Anal Chem 2020;125:115842.
3. Naseri M, Ziora ZM, Simon GP, Batchelor W. ASSURED-compliant point-of-care diagnostics for the detection of human viral infections. Rev Med Virol 2022;32:e2263.
4. Otoo JA, Schlappi TS. REASSURED multiplex diagnostics: A critical review and forecast. Biosensors (Basel) 2022;12:124.
5. Sailapu SK, Liébana S, Merino-Jimenez I, Esquivel JP, Sabaté N. Towards a REASSURED reality: A less-is-more electronic design strategy for self-powered glucose test. Biosens Bioelectron 2024;243:115708.
6. Mirica AC, Stan D, Chelcea IC, Mihailescu CM, Ofiteru A, Bocancia-Mateescu LA. Latest trends in lateral flow immunoassay (LFIA) detection labels and conjugation process. Front Bioeng Biotechnol 2022;10:922772.
7. Parolo C, Sena-Torralba A, Bergua JF, Calucho E, Fuentes-Chust C, Hu L, et al. Tutorial: Design and fabrication of nanoparticle-based lateral-flow immunoassays. Nat Protoc 2020;15:3788-816.
8. Koczula KM, Gallotta A. Lateral flow assays. Essays Biochem 2016;60:111-20.
9. Bahadır EB, Sezgintürk MK. Lateral flow assays: Principles, designs and labels. TrAC Trends Anal Chem 2016;82:286-306.
10. Pedreira-Rincón J, Rivas L, Comenge J, Skouridou V, Camprubí-Ferrer D, Muñoz J, et al. A comprehensive review of competitive lateral flow assays over the past decade. Lab Chip 2025;25:2578-608.
11. Li D, Huang M, Shi Z, Huang L, Jin J, Jiang C, et al. Ultrasensitive competitive lateral flow immunoassay with visual semiquantitative inspection and flexible quantification capabilities. Anal Chem 2022;94:2996-3004.
12. Andryukov BG. Six decades of lateral flow immunoassay: From determining metabolic markers to diagnosing COVID-19. AIMS Microbiol 2020;6:280-304.
13. Ross GM, Filippini D, Nielen MW, Salentijn GI. Unraveling the hook effect: A comprehensive study of high antigen concentration effects in Sandwich lateral flow immunoassays. Anal Chem 2020;92:15587-95.
14. Sathishkumar N, Toley BJ. Development of an experimental method to overcome the hook effect in sandwich-type lateral flow immunoassays guided by computational modelling. Sens Actuators B Chem 2020;324:128756.
15. Khelifa L, Hu Y, Jiang N, Yetisen AK. Lateral flow assays for hormone detection. Lab Chip 2022;22:2451-75.
16. Kim H, Chung DR, Kang M. A new point-of-care test for the diagnosis of infectious diseases based on multiplex lateral flow immunoassays. Analyst 2019;144:2460-6.
17. Gupta Y, Ghrera AS. Recent advances in gold nanoparticle-based lateral flow immunoassay for the detection of bacterial infection. Arch Microbiol 2021;203:3767-84.
18. Ince B, Sezgintürk MK. Lateral flow assays for viruses diagnosis: Up-to-date technology and future prospects. Trends Analyt Chem 2022;157:116725.
19. Sohrabi H, Majidi MR, Fakhraei M, Jahanban-Esfahlan A, Hejazi M, Oroojalian F, et al. Lateral flow assays (LFA) for detection of pathogenic bacteria: A small point-of-care platform for diagnosis of human infectious diseases. Talanta 2022;243:123330.
20. Huang L, Tian S, Zhao W, Liu K, Ma X, Guo J. Multiplexed detection of biomarkers in lateral-flow immunoassays. Analyst 2020;145:2828-40.
21. Shen M, Li N, Lu Y, Cheng J, Xu Y. An enhanced centrifugation-assisted lateral flow immunoassay for the point-of-care detection of protein biomarkers. Lab Chip 2020;20:2626-34.
22. Patil AA, Kaushik P, Jain RD, Dandekar PP. Assessment of urinary biomarkers for infectious diseases using lateral flow assays: A comprehensive overview. ACS Infect Dis 2023;9:9-22.
23. Gumus E, Bingol H, Zor E. Lateral flow assays for detection of disease biomarkers. J Pharm Biomed Anal 2023;225:115206.
24. Anfossi L, Baggiani C, Giovannoli C, D'Arco G, Giraudi G. Lateral-flow immunoassays for mycotoxins and phycotoxins: A review. Anal Bioanal Chem 2013;405:467-80.
25. Song S, Liu N, Zhao Z, Njumbe Ediage E, Wu S, Sun C, et al. Multiplex lateral flow immunoassay for mycotoxin determination. Anal Chem 2014;86:4995-5001.
26. Raysyan A, Schneider RJ. Development of a lateral flow immunoassay (LFIA) to screen for the release of the endocrine disruptor bisphenol a from polymer materials and products. Biosensors (Basel) 2021;11:231.
27. Jara MD, Alvarez LA, Guimarães MC, Antunes PW, de Oliveira JP. Lateral flow assay applied to pesticides detection: Recent trends and progress. Environ Sci Pollut Res Int 2022;29:46487-508.
28. Zhang Q, Fang L, Jia B, Long N, Shi L, Zhou L, et al. Optical lateral flow test strip biosensors for pesticides: Recent advances and future trends. TrAC Trends Anal Chem 2021;144:116427.
29. Chowdhury P, Lawrance R, Lu ZY, Lin HC, Chan YH. Recent progress in dual/multi-modal detection modes for improving sensitivity and specificity of lateral flow immunoassays applied for point-of-care diagnostics. TrAC Trends Anal Chem 2024;177:117798.
30. Strohmaier-Nguyen D, Horn C, Baeumner AJ. Innovations in one-step point-of-care testing within microfluidics and lateral flow assays for shaping the future of healthcare. Biosens Bioelectron 2025;267:116795.
31. Willemsen L, Wichers J, Xu M, Van Hoof R, Van Dooremalen C, Van Amerongen A, et al. Biosensing chlorpyrifos in environmental water samples by a newly developed carbon nanoparticle-based indirect lateral flow assay. Biosensors (Basel) 2022;12:735.
32. Wang K, Meng X, Yan X, Fan K. Nanozyme-based point-of-care testing: Revolutionizing environmental pollutant detection with high efficiency and low cost. Nano Today 2024;54:102145.
33. Xing G, Sun X, Li N, Li X, Wu T, Wang F. New advances in lateral flow immunoassay (LFI) Technology for food safety detection. Molecules 2022;27:6596.
34. Wang P, Li J, Guo L, Li J, He F, Zhang H, et al. The developments on lateral flow immunochromatographic assay for food safety in recent 10 years: A review. Chemosensors 2024;12:88.
35. Tang Y, Yuan J, Zhang Y, Khan IM, Ma P, Wang Z. Lateral flow assays based on aptamers for food safety applications. Food Control 2024;155:110051.
36. Abdullaev S, Abomughaid MM, Elawady A, Ibrahim SM, Abd Al Khidhir Abdullah S, Khalid H, et al. Advances in the application of materials in the fabrication of lateral flow assay-based methods for food safety control. Food Rev Int 2024;41:1-24.
37. Linares EM, Kubota LT, Michaelis J, Thalhammer S. Enhancement of the detection limit for lateral flow immunoassays: Evaluation and comparison of bioconjugates. J Immunol Methods 2012;375:264-70.

38. Panferov VG, Zherdev AV, Dzantiev BB. Post-assay chemical enhancement for highly sensitive lateral flow immunoassays: A critical review. Biosensors (Basel) 2023;13:866.
39. Dey MK, Iftesum M, Devireddy R, Gartia MR. New technologies and reagents in lateral flow assay (LFA) designs for enhancing accuracy and sensitivity. Anal Methods 2023;15:4351-76.
40. Fu E, Kauffman P, Lutz B, Yager P. Chemical signal amplification in two-dimensional paper networks. Sens Actuators B Chem 2010;149:325-8.
41. Fu E, Liang T, Houghtaling J, Ramachandran S, Ramsey SA, Lutz B, et al. Enhanced sensitivity of lateral flow tests using a two-dimensional paper network format. Anal Chem 2011;83:7941-6.
42. Tang R, Yang H, Choi JR, Gong Y, Hu J, Feng S, et al. Improved sensitivity of lateral flow assay using paper-based sample concentration technique. Talanta 2016;152:269-76.
43. Tsai TT, Huang TH, Chen CA, Ho NY, Chou YJ, Chen CF. Development a stacking pad design for enhancing the sensitivity of lateral flow immunoassay. Sci Rep 2018;8:17319.
44. Tsai TT, Huang TH, Ho NY, Chen YP, Chen CA, Chen CF. Development of a multiplex and sensitive lateral flow immunoassay for the diagnosis of periprosthetic joint infection. Sci Rep 2019;9:15679.
45. Liu Y, Li J, Xiao Z, Wu T, Zhou C, Zhou J. Microstructure-driven self-transport and convection of water on membrane surface for ultra-fast, highly sensitive, low-cost lateral-flow assays. Small 2024;20:e2309956.
46. Kim W, Lee S, Jeon S. Enhanced sensitivity of lateral flow immunoassays by using water-soluble nanofibers and silver-enhancement reactions. Sens Actuators B Chem 2018;273:1323-7.
47. Preechakasedkit P, Teekayupak K, Citterio D, Ruecha N. Improvement in sensitivity for lateral flow immunoassay of ferritin using novel device design based on gold-enhanced gold nanoparticles. Sci Rep 2022;12:7831.
48. Chien YS, Tsai TT, Lin JH, Chang CC, Chen CF. One-step copper deposition-induced signal amplification for multiplex bacterial infection diagnosis on a lateral flow immunoassay device. Biosens Bioelectron 2025;267:116849.
49. Sena-Torralba A, Álvarez-Diduk R, Parolo C, Piper A, Merkoçi A. Toward next generation lateral flow assays: Integration of nanomaterials. Chem Rev 2022;122:14881-910.
50. Loynachan CN, Thomas MR, Gray ER, Richards DA, Kim J, Miller BS, et al. Platinum nanocatalyst amplification: Redefining the gold standard for lateral flow immunoassays with ultrabroad dynamic range. ACS Nano 2018;12:279-88.
51. Su L, Wang L, Yao X, Yin X, Zhang H, Zhao M, et al. Small size nanoparticles-Co(3)O(4) based lateral flow immunoassay biosensor for highly sensitive and rapid detection of furazolidone. Talanta 2020;211:120729.
52. Kim HM, Kim J, Bock S, An J, Choi YS, Pham XH, et al. Silver-assembled silica nanoparticles in lateral flow immunoassay for visual inspection of prostate-specific antigen. Sensors (Basel) 2021;21:4099.
53. Liang M, Cai X, Gao Y, Yan H, Fu J, Tang X, et al. A versatile nanozyme integrated colorimetric and photothermal lateral flow immunoassay for highly sensitive and reliable Aspergillus flavus detection. Biosens Bioelectron 2022;213:114435.
54. Hao L, Yang W, Xu Y, Cui T, Zhu G, Zeng W, et al. Engineering light-initiated afterglow lateral flow immunoassay for infectious disease diagnostics. Biosens Bioelectron 2022;212:114411.
55. Liu S, Dou L, Yao X, Zhang W, Zhao M, Yin X, et al. Nanozyme amplification mediated on-demand multiplex lateral flow immunoassay with dual-readout and broadened detection range. Biosens Bioelectron 2020;169:112610.
56. Gong H, Gai S, Tao Y, Du Y, Wang Q, Ansari AA, et al. Colorimetric and photothermal dual-modal switching lateral flow immunoassay based on a forced dispersion prussian blue nanocomposite for the sensitive detection of prostate-specific antigen. Anal Chem 2024;96:8665-73.
57. Miller BS, Bezinge L, Gliddon HD, Huang D, Dold G, Gray ER, et al. Spin-enhanced nanodiamond biosensing for ultrasensitive diagnostics. Nature 2020;587:588-93.
58. Bai Z, Wei H, Yang X, Zhu Y, Peng Y, Yang J, et al. Rapid enrichment and ultrasensitive detection of influenza a virus in human specimen using magnetic quantum dot nanobeads based test strips. Sens Actuators B Chem 2020;325:128780.
59. Zhang X, Zhao F, Sun Y, Mi T, Wang L, Li Q, et al. Development of a highly sensitive lateral flow immunoassay based on receptor-antibody-amorphous carbon nanoparticles to detect 22 β-lactams in milk. Sens Actuators B Chem 2020;321:128458.
60. Brosamer K, Kourentzi K, Willson RC, Vu BV. Glowstick-inspired smartphone-readable reporters for sensitive, multiplexed lateral flow immunoassays. Commun Eng 2023;2:31.
61. Dang M, Li Z, Mao Y, Huang X, Song L, Li W, et al. A highly sensitive lateral flow immunoassay based on a group-specific monoclonal antibody and amorphous carbon nanoparticles for detection of sulfonamides in milk. Mikrochim Acta 2023;190:186.
62. Jin B, Du Z, Ji J, Bai Y, Tang D, Qiao L, et al. Regulation of probe density on upconversion nanoparticles enabling high-performance lateral flow assays. Talanta 2023;256:124327.
63. Jung H, Park SH, Lee J, Lee B, Park J, Seok Y, et al. A size-selectively biomolecule-immobilized nanoprobe-based chemiluminescent lateral flow immunoassay for detection of avian-origin viruses. Anal Chem 2021;93:792-800.
64. Wu L, Zhu Z, Xue J, Zheng L, Liu H, Ouyang H, et al. Chemiluminescent/photothermal dual-mode lateral flow immunoassay based on CoFe PBAs/WS2 nanozyme for rapid and highly sensitive point-of-care testing of gentamicin. Biosens Bioelectron 2024;265:116711.
65. John Frederick William H. On a case of superficial colour presented by a homogeneous liquid internally colourless. Philos Trans R S Lond 1845;135:143-5.
66. Zacharioudaki DE, Fitilis I, Kotti M. Review of fluorescence spectroscopy in environmental quality applications. Molecules 2022;27:4801.
67. Zhong W. Nanomaterials in fluorescence-based biosensing. Anal Bioanal Chem 2009;394:47-59.
68. Chandra A, Prasad S, Gigli G, del Mercato LL. Chapter 6 – Fluorescent nanoparticles for sensing. In: Parak WJ, Feliu N, editors. Frontiers of Nanoscience. Amsterdam: Elsevier; 2020. p. 117-49.
69. Zhao L, Xu J, Xiong L, Wang S, Yu C, Lv J, et al. Recent development of chemiluminescence for bioanalysis. TrAC Trends Anal Chem 2023;166:117213.
70. Wang H, Wan K, Shi X. Recent advances in nanozyme research. Adv Mater 2019;31:e1805368.
71. Wang Q, Wei H, Zhang Z, Wang E, Dong S. Nanozyme: An emerging alternative to natural enzyme for biosensing and immunoassay. TrAC Trends in Anal Chem 2018;105:218-24.
72. Li S, Zhang Y, Wang Q, Lin A, Wei H. Nanozyme-enabled analytical chemistry. Anal Chem 2022;94:312-23.
73. Zhang D, Huang L, Liu B, Ni H, Sun L, Su E, et al. Quantitative and ultrasensitive detection of multiplex cardiac biomarkers in lateral flow assay with core-shell SERS nanotags. Biosens Bioelectron 2018;106:204-11.
74. Jia X, Wang K, Li X, Liu Z, Liu Y, Xiao R, et al. Highly sensitive detection of three protein toxins via SERS-lateral flow immunoassay based on SiO(2)@Au nanoparticles. Nanomedicine 2022;41:102522.
75. González-Cabaleiro L, Fernández-Lodeiro C, Vázquez-Iglesias L, Soriano-Maldonado P, van Raaij MJ, Bodelón G, et al. Pushing the limits of lateral flow immunoassay by digital SERS for the ultralow detection of SARS-CoV-2 virus. Small Sci 2024;4:2400259.
76. Lee KW, Kim KR, Chun HJ, Jeong KY, Hong DK, Lee KN, et al. Time-resolved fluorescence resonance energy transfer-based lateral flow immunoassay using a raspberry-type europium particle and a single

membrane for the detection of cardiac troponin I. Biosens Bioelectron 2020;163:112284.

77. Zhang X, Ding M, Mao Y, Huang X, Xie X, Song L, et al. A comparative study of "turn-off" mode and "turn-on" mode lateral flow immunoassay for T-2 toxin detection. Sens Actuators B Chem 2022;359:131545.
78. Wang Y, Qin Z, Boulware DR, Pritt BS, Sloan LM, González IJ, et al. Thermal contrast amplification reader yielding 8-fold analytical improvement for disease detection with lateral flow assays. Anal Chem 2016;88:11774-82.
79. Zhan L, Granade T, Liu Y, Wei X, Youngpairoj A, Sullivan V, et al. Development and optimization of thermal contrast amplification lateral flow immunoassays for ultrasensitive HIV p24 protein detection. Microsyst Nanoeng 2020;6:54.
80. Shirshahi V, Tabatabaei SN, Hatamie S, Saber R. Photothermal enhancement in sensitivity of lateral flow assays for detection of *E-coli* O157:H7. Colloids Surf B Biointerfaces 2020;186:110721.
81. Liu Y, Zhan L, Kangas J, Wang Y, Bischof J. Fast and ultrafast thermal contrast amplification of gold nanoparticle-based immunoassays. Sci Rep 2022;12:12729.
82. Han XX, Rodriguez RS, Haynes CL, Ozaki Y, Zhao B. Surface-enhanced raman spectroscopy. Nat Rev Methods Primers 2022;1:87.
83. Hang Y, Boryczka J, Wu N. Visible-light and near-infrared fluorescence and surface-enhanced Raman scattering point-of-care sensing and bio-imaging: A review. Chem Soc Rev 2022;51:329-75.
84. Ma L, Yang F, Zheng J. Application of fluorescence resonance energy transfer in protein studies. J Mol Struct 2014;1077:87-100.
85. Xu S, Bai X, Wang L. Exploration of photothermal sensors based on photothermally responsive materials: A brief review. Inorg Chem Front 2018;5:751-9.
86. Zong C, Xu M, Xu LJ, Wei T, Ma X, Zheng XS, et al. Surface-enhanced raman spectroscopy for bioanalysis: Reliability and challenges. Chem Rev 2018;118:4946-80.
87. Ding SY, Yi J, Li JF, Ren B, Wu DY, Panneerselvam R, et al. Nanostructure-based plasmon-enhanced Raman spectroscopy for surface analysis of materials. Nat Rev Mater 2016;1:16021.
88. Förster T. Zwischenmolekulare Energiewanderung und Fluoreszenz. Ann Phys 1948;437:55-75.
89. Yang WC, Li SY, Ni S, Liu G. Advances in FRET-based biosensors from donor-acceptor design to applications. Aggregate 2024;5:e460.
90. Imani M, Mohajeri N, Rastegar M, Zarghami N. Recent advances in FRET-Based biosensors for biomedical applications. Anal Biochem 2021;630:114323.
91. Ye H, Liu Y, Zhan L, Liu Y, Qin Z. Signal amplification and quantification on lateral flow assays by laser excitation of plasmonic nanomaterials. Theranostics 2020;10:4359-73.
92. Li C, Wu Y, Wang Y, Jiao J, Li D, Liu Q. Recent advances in the detection of various biomarkers by lateral flow immunoassay: From hazardous substances to *in vitro* diagnosis. Coord Chem Rev 2025;545:217037.
93. Banerjee R, Jaiswal A. Recent advances in nanoparticle-based lateral flow immunoassay as a point-of-care diagnostic tool for infectious agents and diseases. Analyst 2018;143:1970-96.
94. Boehringer HR, O'Farrell BJ. Lateral flow assays in infectious disease diagnosis. Clin Chem 2021;68:52-8.
95. Deng Y, Jiang H, Li X, Lv X. Recent advances in sensitivity enhancement for lateral flow assay. Mikrochim Acta 2021;188:379.
96. Liu Y, Zhan L, Qin Z, Sackrison J, Bischof JC. Ultrasensitive and highly specific lateral flow assays for point-of-care diagnosis. ACS Nano 2021;15:3593-611.